

1. Aims and purposes of the satellite

Extreme earthquake is one of the worst disasters in countries near the plate boundaries on earth, such as Japan and Taiwan. Based on global statistics from USGS (U.S. Geological Survey), earthquakes of magnitude higher than 7.0 occur 11~20 times per year in last ten years (Figure 1).

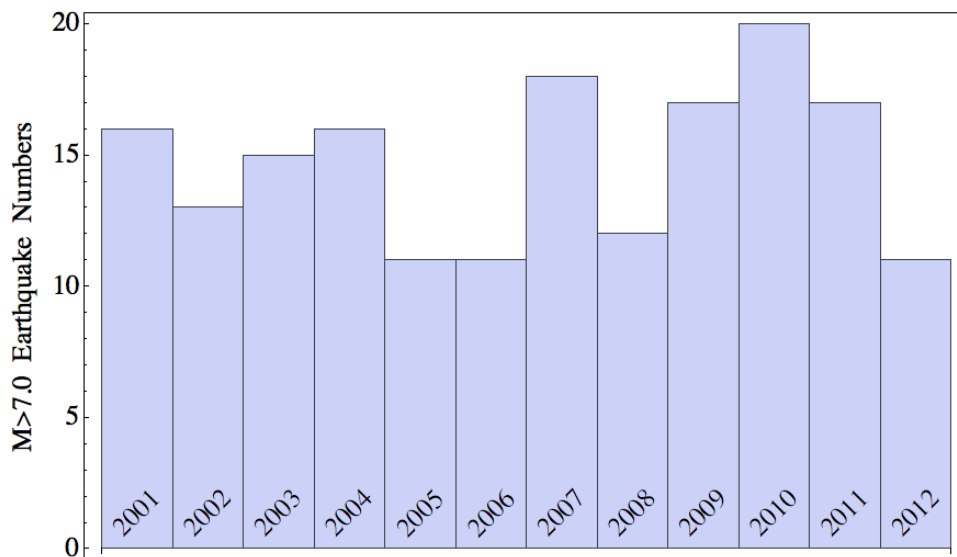


Figure 1. Numbers of M>7.0 Earthquake in Last Ten Years

Possible earthquake precursor effects on ionosphere have been reported by many scientists [1][7]. Even though the morphology of the ionosphere disturbances caused by large earthquakes is still not clear, more and more ground-based observation data analyses as well as satellite data analyses in this research area show convincing results on such precursor effect on ionosphere [8][16]. While more satellite data are still needed for this study [17][19].

The main purpose of the CKUSAT mission is to provide accurate and reliable data at proper height and latitude region for the study of ionosphere disturbances due to large earthquakes. Hence, the CKUSAT will carry three scientific payloads: Impedance Probe (IP), Electron Temperature Probe (ETP) and Very-Low Frequency (VLF) sensor. An IP for absolute electron density measurement is used for studies of latitude and longitude distribution of plasma density anomaly before large earthquakes [20]. An ETP for accurate electron temperature measurement is used for studies of reduction of electron temperature in low-latitude ionosphere before and after large earthquakes. A VLF sensor is used for monitoring the electric field disturbances before large earthquakes for mechanism studies of these ionosphere disturbances [21]. In addition to the earthquake research, the CKUSAT development will intend to encourage the space engineering education and engineering application for participated students to gain hands-on experience such as satellite bus and experimental space-borne GPS receiver payload. All the satellite subsystems and payloads will be primarily developed domestically using commercial-off-the-shelf components to reduce the satellite cost and build up the university capability in microsatellite development.

However, only one satellite cannot provide a global coverage and routine observation, a constellation is recommend and needed for the earthquake precursor studies as well as a global earthquake warning system development in the future. (e.g. 4~5 satellites with 5 degree longitude

separation at the same height). Modular design architecture is important factor to construct a satellite constellation equip with the same scientific payloads. We hope the CKUSAT could be a pioneer to show that a university is affordable and capable to design and develop a microsatellite. Hence, it will also stimulate global universities to join the international cooperation mission to form an earthquake precursor constellation.

2. Design result

2.1 CKUSAT system

The CKUSAT system mainly consists of three segments, which space segment, ground segment, and launch segment (Figure 2). The term, space segment, is also called as spacecraft which refers to the CKUSAT microsatellite. The CKUSAT microsatellite includes six subsystems, three scientific payloads and two experimental payloads. In addition to the space segment, the ground segment would also mainly be constructed and operated by NCKU team. According to the design constraint, the launch segment is the JAXA H-IIA launch vehicle piggy-back.

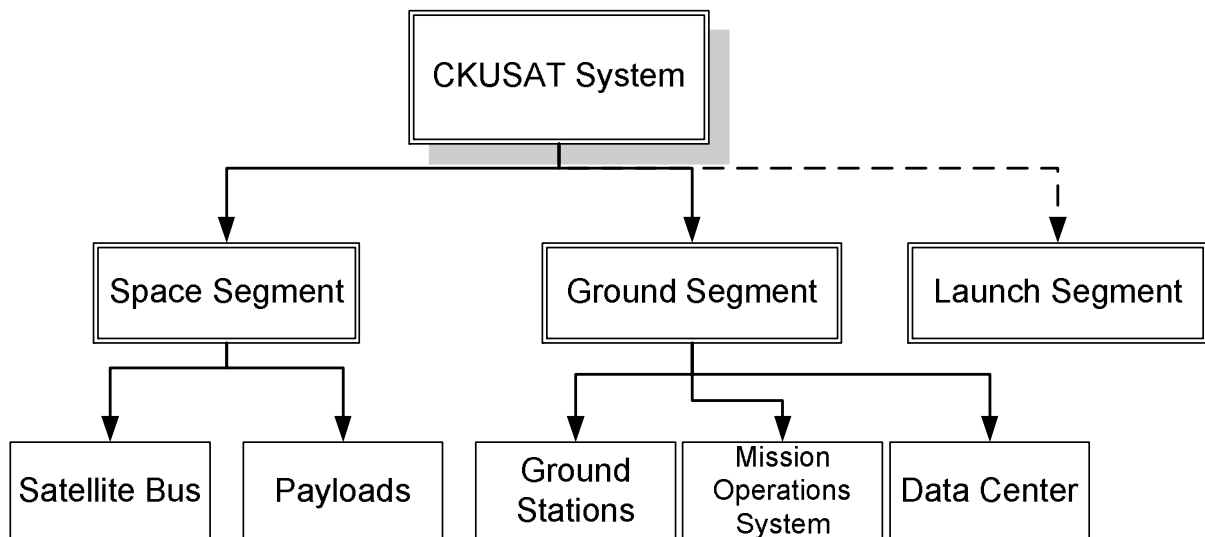


Figure 2. CKUSAT System Element

The six subsystems are: Structure and Mechanisms Subsystem (SMS), Thermal Control Subsystem (TCS), Attitude Determination and Control Subsystem (ADCS), Electrical and Power Subsystem (EPS), Telemetry and Tracking and Command subsystem (TT&C), and Command and Data Handling subsystem (C&DH). The five payloads include the Electron Temperature Probe (ETP), the Impedance Probe (IP), the Very-Low Frequency sensor (VLF), the GPS Receiver for space application (GPSR), and the Experiment for Communication Payload (ECP). The system organization is shown as follow.

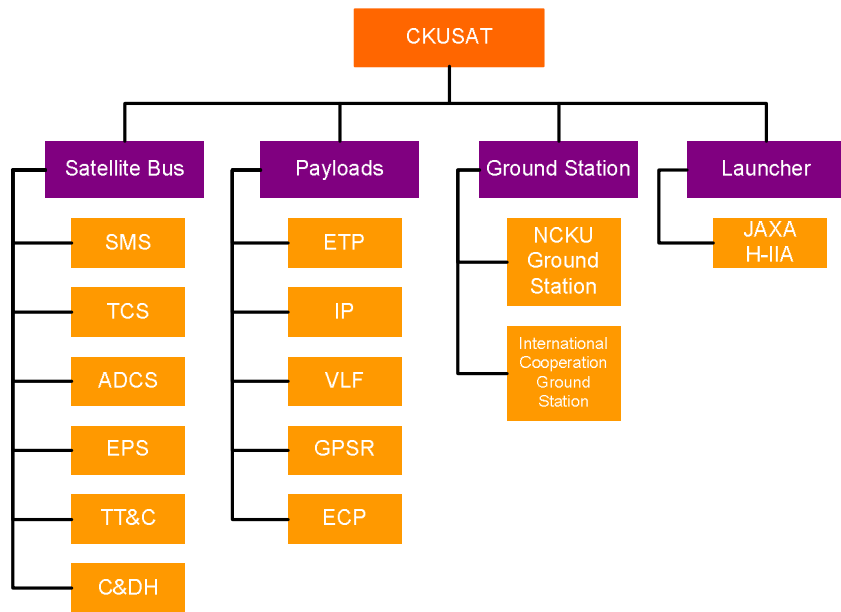


Figure 3. CKUSAT System Organization

Since plasma density and electron temperature are disturbed most at lower latitude region. Many large earthquakes also occur at low latitude (Figure 4), so that CKUSAT orbit is chosen nearly circular with inclination of 35 degrees. Considering ionosphere disturbances is clearer at low altitude as well as satellite life and low-altitude wind system, satellite orbit altitude is chosen as 500 km. The orbit simulation renders the satellite coverage and the ground contacts as shown in Figure 5. The orbit period is about 94.6 minutes and the average pass duration is about 630 seconds. Moreover, the time-scale of ionosphere disturbances before large earthquakes is 4~5 days, space-scale is about 70 degree longitude and 20 degree latitude. Based on previous earthquakes statistics of USGS, we expect CKUSAT being able to study at least 5~10 global ionospheric earthquake precursor events in one year.

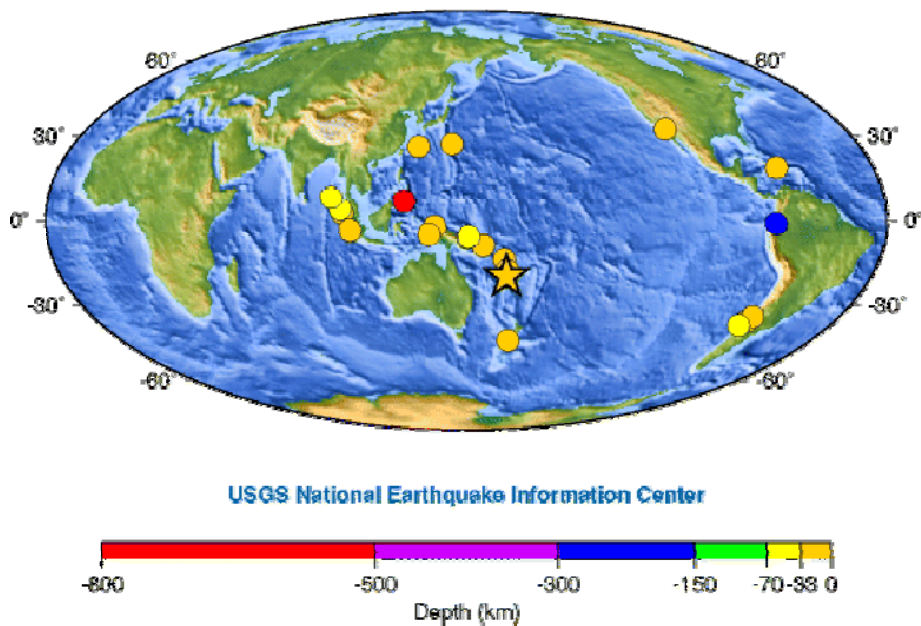


Figure 4. Earthquakes Magnitude 7.0 and Greater in 2010

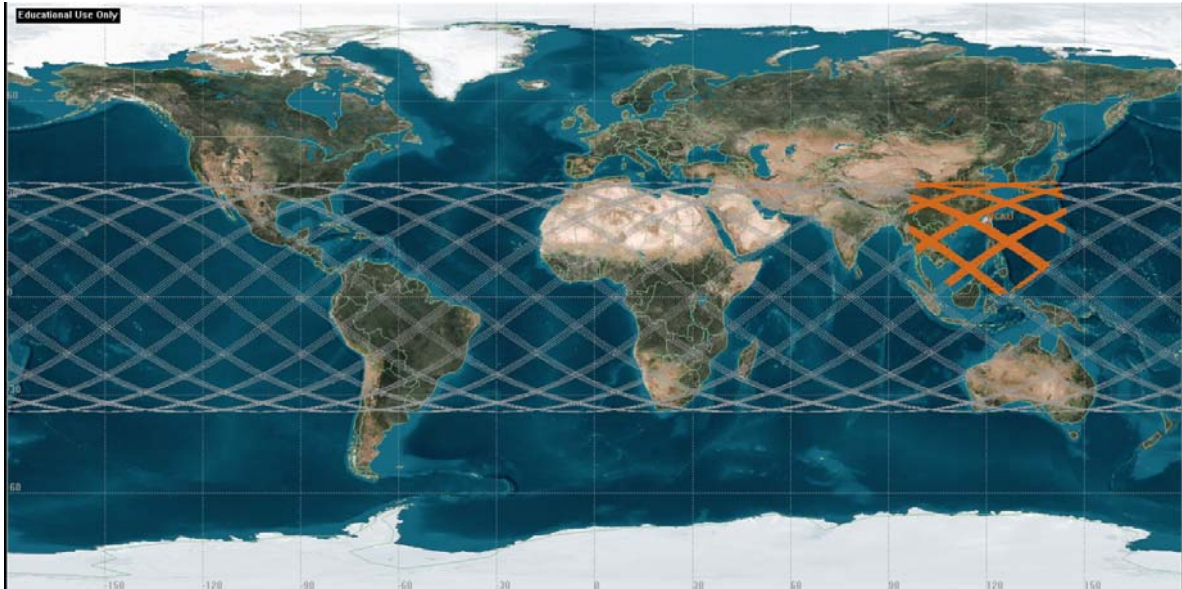


Figure 5. CKUSAT Satellite Orbit Simulation

In order to provide the modular design architecture, the building block is the main idea of the CKUSAT satellite configuration. The circuit board of satellite subsystem/payload would be located inside a 12cm x 7.5cm basic module, which is then fixed on the satellite frame (Figure 6). There will then be six basic modules to form a basic unit. The CKUSAT consists of two basic units and its configuration is shown in Figure 7. The lower unit will mainly be satellite bus modules, such as ADCS, EPS, C&DH, TT&C. In addition to subsystem module, the ETP & IP module, battery module, and reaction wheel are located in the lower unit. The upper unit will equip the payload circuit modules, which are VLF and GPSR (Figure 8). The body six side faces are mounted with solar cells and the panels will be deployed for getting more sunlight power. Because of ECP communication requirement, the bottom face, which equips the ECP S-band patch antenna, will point to the earth. Consequently, the GPS antennas and VLF sensor will be attached on the top panel. In addition, the electrode probe of ETP and IP will face the ram direction of CKUSAT flight according to the requirement of ECP and IP payloads.

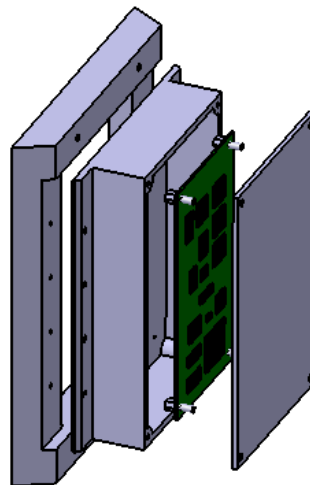


Figure 6. CKUSAT Basic Module

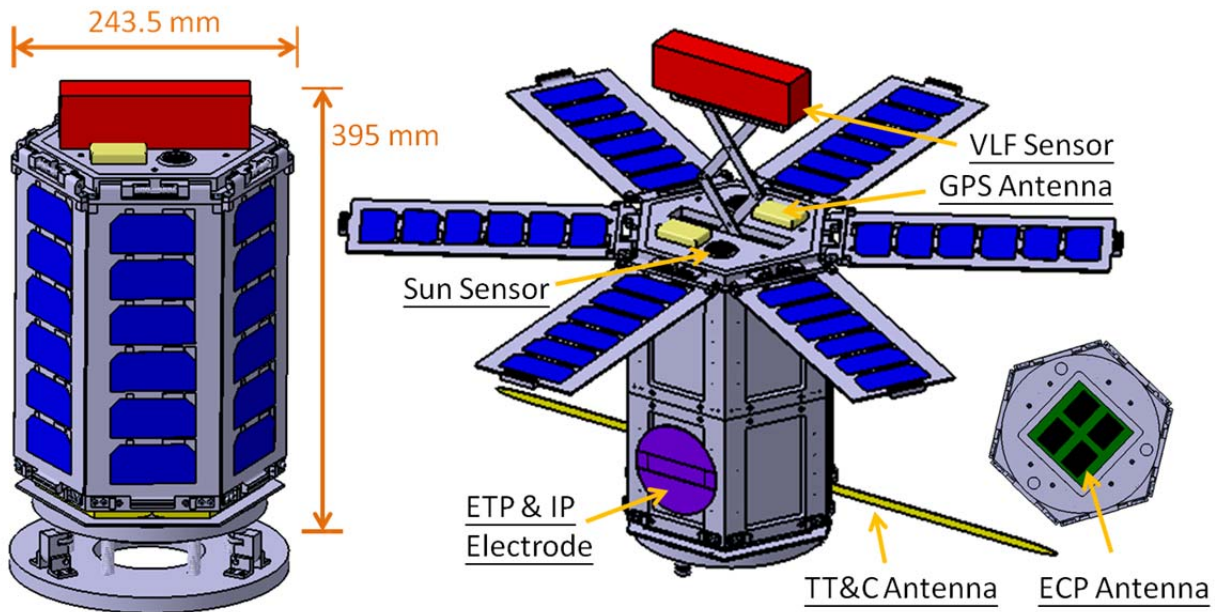


Figure 7. CKUSAT Satellite Configuration

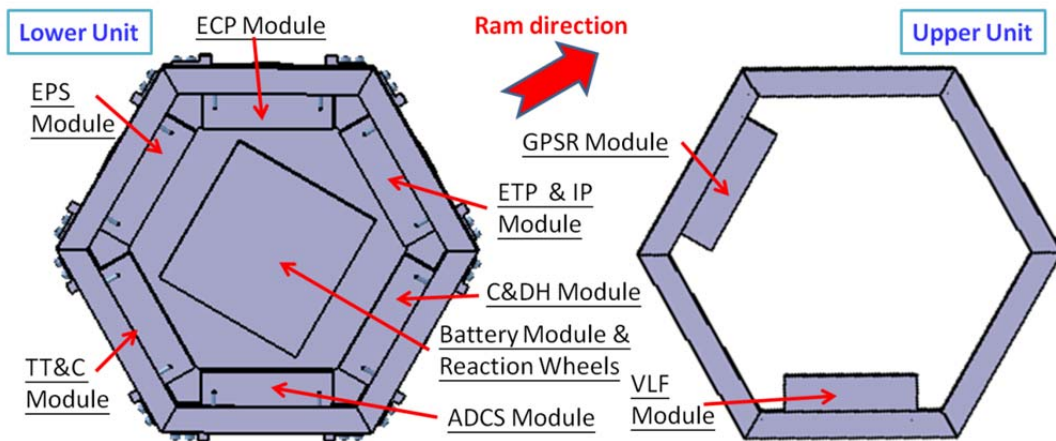


Figure 8. CKUSAT Satellite Inner Configuration

The electrical energy shall be provided by the surface mounted solar cells and the rechargeable batteries. The power budget of the CKUSAT satellite is shown in Table 1. The total power consumption is about 10.9W, and the available generated power is about 11.4W according to the result of power generation analysis (Figure 9). Hence, the power of solar cells can fulfill the satellite operation requirement. According to the satellite design contest constrains, the CKUSAT satellite total weight at launch doesn't exceed 50 kg and the dimension of CKUSAT satellite at launch doesn't exceed 50 cm³. The mass budget of the CKUSAT satellite is depicted in Table 2. The mass and configuration of the CKUSAT satellite can then fulfill design constrain.

Table 1. CKUSAT Power Budget

	Estimate Avg. Power (W)	
SubSystem	4.800	42.48%
ADCS	1.50	13.27%
C&DH	1.30	11.50%
EPS	0.30	2.65%
TCS	0.20	1.77%
TT&C	1.50	13.27%
Payload	6.500	15.93%
ECP	4.40	38.94%
GPSR	0.80	7.08%
ETP	0.50	4.42%
IP	0.50	4.42%
VLF	0.30	2.65%
Total	11.30	
Avaiable	11.40	

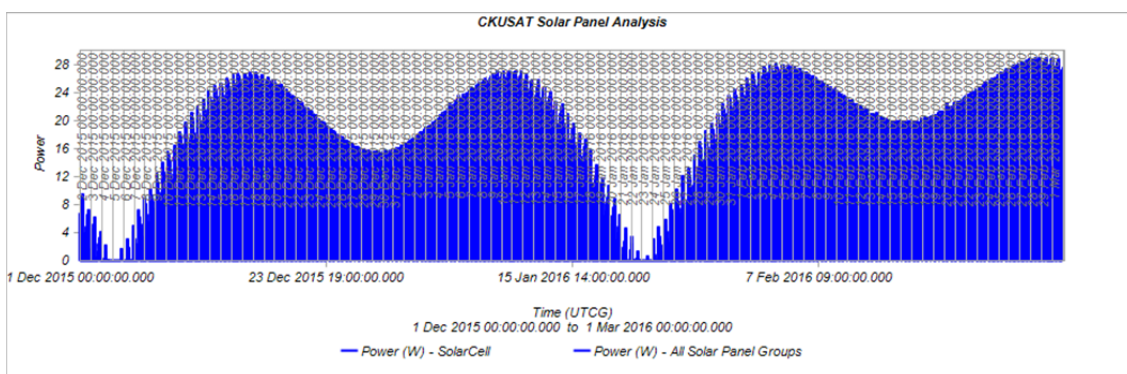
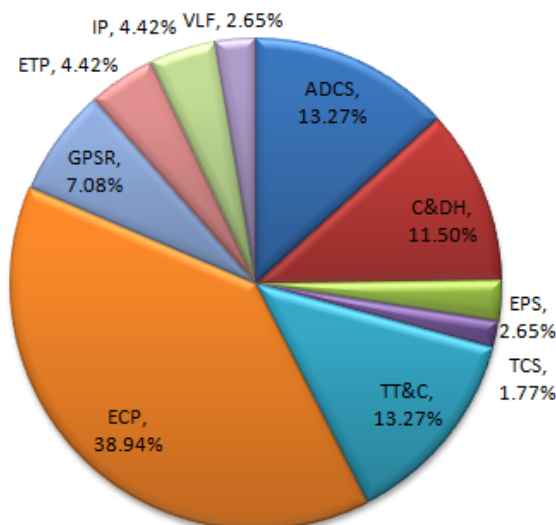


Figure 9. CKUSAT Solar Power Generation Simulation

Table 2. CKUSAT Mass Budget

Components	Mass Allocation(g)	Percentage	Notes
Bus			
SMS	5000	35.97%	Deployment fixture included Reaction wheel included Battery module included
TCS	200	1.44%	
ADCS	2000	14.39%	
EPS	1000	7.19%	
TT&C	500	3.60%	
C&DH	600	4.32%	
Payload			
ECP	600	4.32%	
GPSR	600	4.32%	
ETP	500	3.60%	
IP	500	3.60%	
VLF	1200	8.63%	
Misc			
Harness	300	2.16%	Included in total mass.
Adaptor	900	6.47%	
Total Mass	13900	100.00%	
Goal	15000		
Margin	1100	7.33%	

The CKUSAT communication will use amateur radio UHF band with data rate 9600bps and link budget are shown in the following.

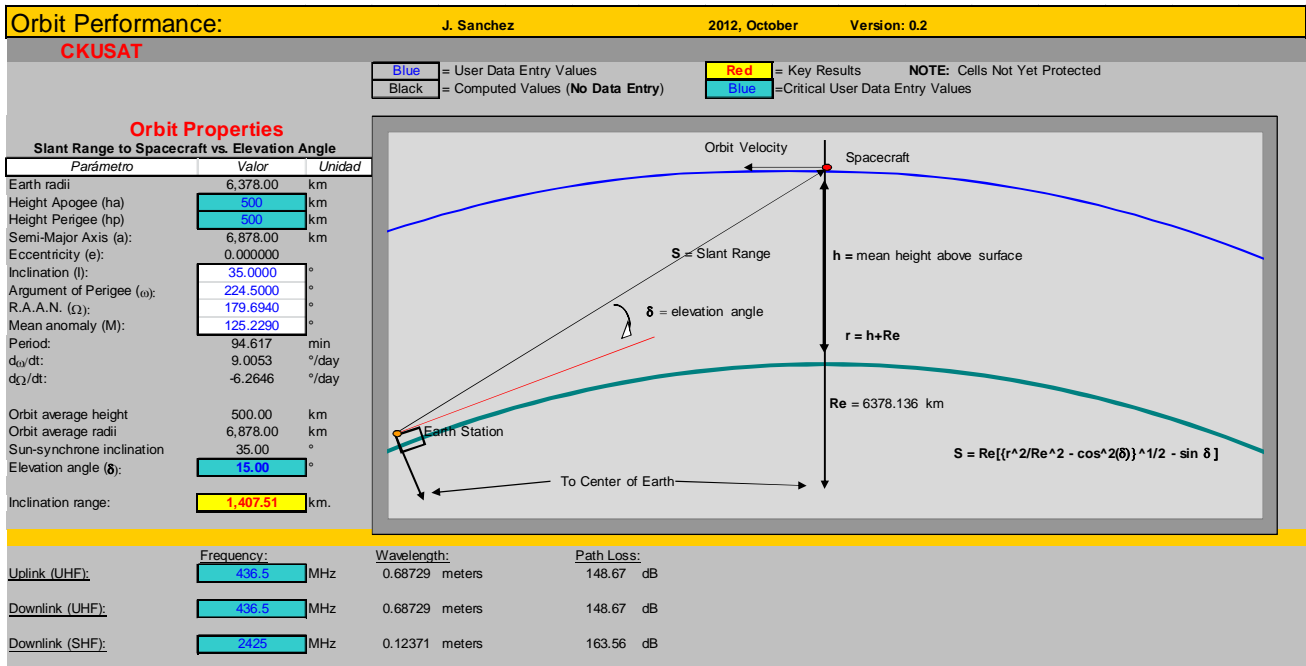


Figure 10. CKUSAT Link Budget Settings

Table 3. Link Budget - Downlink(Left) / Uplink(Right)

Parameter:	Value:	Units:	Parameter:	Value:	Units:
Spacecraft:			Ground Station:		
Transmitter Power Output:	0.75	watts	Transmitter Power Output:	5.0	watts
	In dBW:	-1.25 dBW		In dBW:	7.0 dBW
	In dBm:	28.75 dBm		In dBm:	37.0 dBm
Transmission Line Losses:	-0.5	dB	Transmission Line Losses:	-2.00	dB
Connector, Filter or In-Line Switch Losses:	-1.0	dB	Connector, Filter or In-Line Switch Losses:	-1.0	dB
Antenna Gain:	2.15	dBiC	Antenna Gain:	16.15	dBiC
Satellite EIRP:	-0.60	dBW	Ground Station EIRP:	20.1	dBW
Downlink Path:			Uplink Path:		
Satellite Antenna Pointing Loss:	-7.0	dB	Ground Station Antenna Pointing Loss:	-3.0	dB
Antenna Polarization Losses:	0.0	dB	Antenna Polarization Losses:	-3.0	dB
Path Loss:	-148.67	dB	Path Loss:	-148.67	dB
Atmospheric Losses:	-0.5	dB	Atmospheric Losses:	-0.5	dB
Ionospheric Losses:	-0.2	dB	Ionospheric Losses:	-0.2	dB
Rain Losses:	0.0	dB	Rain Losses:	0.0	dB
Isotropic Signal Level at Ground Station:	-156.97	dBW	Isotropic Signal Level at Satellite:	-135.23	dBW
Ground Station:			Spacecraft:		
----- Eb/No -----			----- Eb/No -----		
Ground Station Antenna Pointing Loss:	-3.0	dB	Spacecraft Antenna Pointing Loss:	-7.0	dB
Ground Station Antenna Gain:	14.9	dBiC	Spacecraft Antenna Gain:	12.60	dBiC
Ground Station Transmission Line Losses:	-0.5	dB	Spacecraft Transmission Line Losses:	-0.50	dB
Ground Station LNA Noise Temperature:	66.7779435	K	Spacecraft LNA Noise Temperature:	169.6	K
Ground Station Transmission Line Temp.:	290	K	Spacecraft Transmission Line Temp.:	270	K
Ground Station Sky Temperature:	450	K	Spacecraft Sky Temperature:	290	K
S/C Transmission Line Coefficient:	0.8913		S/C Transmission Line Coefficient:	0.8913	
Ground Station Effective Noise Temperature:	499	K	Spacecraft Effective Noise Temperature:	457	K
Ground Station Figure of Merit (G/T):	-12.6	dB/K	Spacecraft Figure of Merit (G/T):	-13.5	dB/K
S/C Signal-to-Noise Power Density (S/No):	56.0	dBHz	S/C Signal-to-Noise Power Density (S/No):	72.9	dBHz
System Desired Data Rate:	9600	bps	System Desired Data Rate:	9600	bps
	In dBHz:	39.8 dBHz		In dBHz:	39.8 dBHz
Telemetry System Eb/No:	16.2	dB	Telemetry System Eb/No:	33.0	dB
Telemetry System Required Bit Error Rate:	1.00E-05		Telemetry System Required Bit Error Rate:	1.00E-05	
Telemetry System Required Eb/No:	13	dB	Telemetry System Required Eb/No:	13.0	dB
System Link Margin:	3.2	dB	System Link Margin:	20.0	dB

Figure 11 shows the CKUSAT operation modes, which are launch mode, initialization mode, detumbling mode, normal mode, safety mode, and contact mode. During the satellite launch phase,

the satellite will be powered off and installed in the launcher. After the satellite separates from the launcher, the main power bus will connect the solar array power and the battery power to start and initialize the CKUSAT satellite. After the initialization mode, the satellite will transfer to the detumbling mode, which means that the magnetic control function will be started by the flight software to stabilize the satellite. At the same time, the satellite also transmits the SOH data in Morse code format via TT&C subsystem for ground station tracking. In the normal mode, the satellite will execute the flight software according to the uplink telecommands and schedule. In addition, the CKUSAT will provide the broadcast signal to world-wide amateur users. However, the satellite will return to the detumbling mode for satellite stabilization, when angular rate of the satellite is larger than a threshold. When the voltage is below than a pre-determined threshold, the detector will generate an interrupt to the onboard processor for safety mode transition. The flight software will turn off the non-essential loads and disable the attitude control to save the power and charge the batteries. When CKUSAT executes the contact operation, the TM transceiver is already powered on to the correct operating frequency and the beacon transmitter is powered off. TT&C subsystem is standby to receive commands or transmit telemetry. In addition, the CKUSAT will perform the ECP experiment depending on the power condition in the contact mode.

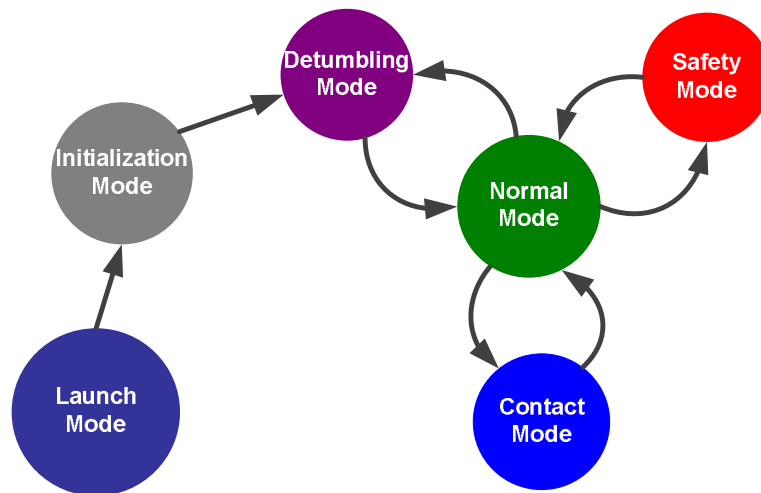


Figure 11. Operation Modes and Mode Transition

2.2 Satellite design

Structure and Mechanisms Subsystem (SMS)

The preliminary SMS design is performed and intended to fulfill the configuration, mass and center of gravity requirements. Below is the SMS design flowchart (Figure 12). The initial satellite configuration design will be dealt with CATIA software. The design was put into considerations of requirements such as center of gravity, moment of inertia, and weight. After the structure design, the next step is going into finite element model created and analysis process. The structure analysis will be conducted to make sure the CKUSAT satellite could survive in launch and space environment. The analysis process includes parameters setting, modeling, meshing, boundary conditions applying, solving and post-processing.

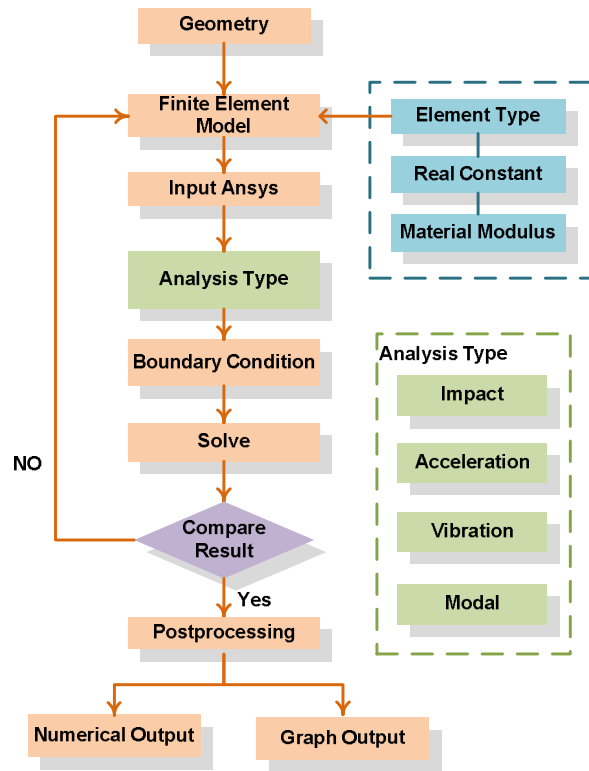


Figure 12. SMS Design Flowchart

ANSYS software is used to build up the CKUSAT finite element model (Figure 13) and analyses, such as modal, acceleration and vibration. There are five modes of CKUSAT below 2000 HZ, which are shown in the following figures.

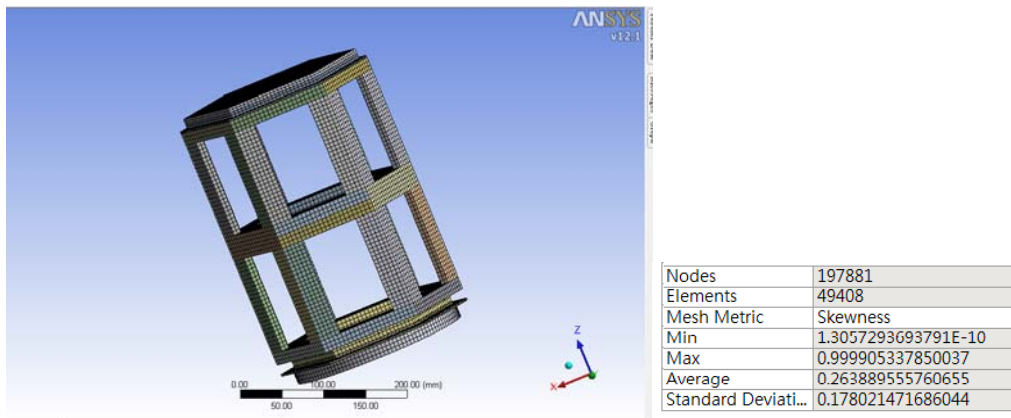


Figure 13. CKUSAT Finite Element Model

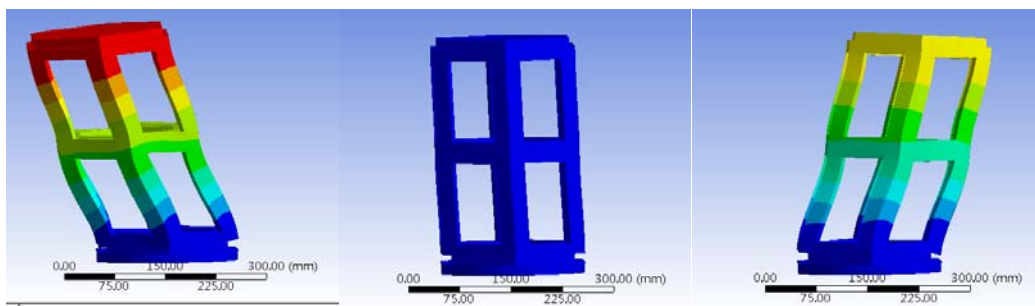


Figure 14. Bending Mode: 323.84 Hz

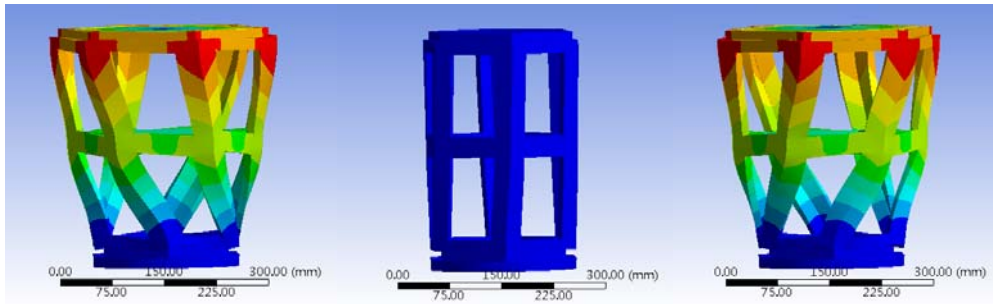


Figure 15. Torsion Mode: 576.3 Hz

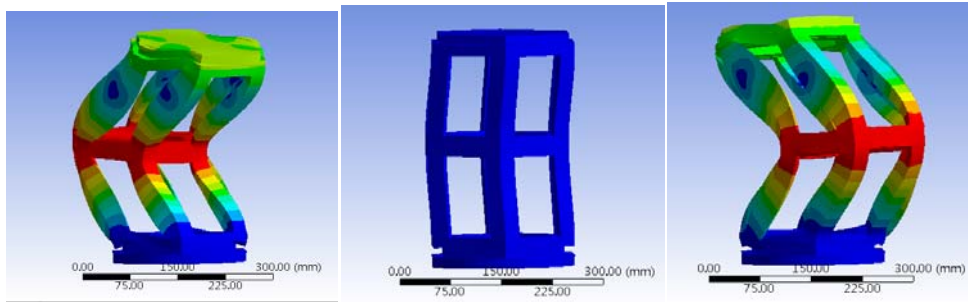


Figure 16. 2nd Bending Mode: 1068.6 Hz

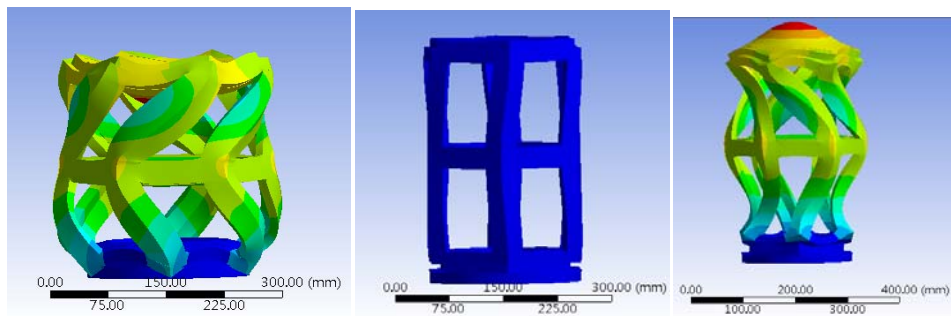


Figure 17. 2nd Torsion Mode: 1633.0 Hz

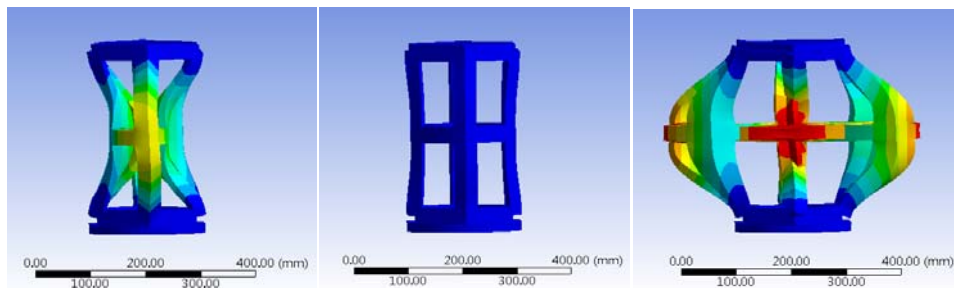


Figure 18. Breathing Mode: 1889.8 Hz

In addition to modal analysis, more analyses should be done according to the H-IIA launch vehicle parameters to make sure the CKUSAT can satisfy the launch environment (Table 4). After analysis process, the CKUSAT should do the environment test to confirm the analyses.

Table 4. H-IIA Launcher Parameters

Quasi-Static Acceleration

	Longitudinal	Lateral
Compression	-6 g	±5 g
Tension	5 g	±5 g

Sine Wave Vibration

	Frequency	Acceleration
Longitudinal	5-100	2.5 g
Lateral	5-100	2 g

Random Vibration

Frequency Width(Hz)	Acceleration (g^2/Hz)
20-200	+3 (dB/octave)
200-2000	0.032
Actual	7.8 (Grms)

Thermal Control Subsystem (TCS)

The CKUSAT thermal control is mainly passive. However, active thermal devices, heaters or cooling devices, will be employed while temperature of any component drops below the allowable range. In the TCS analysis flowchart (Figure 19), team members will obtain orbit information, simulate heat flux, build satellite thermal model, and determine the radiation exchange factors and view factors to obtain the thermal simulation results. Passive thermal control will be adopted according to thermal analysis results, for examples, providing appropriate thermal insulation and selecting the proper material properties.

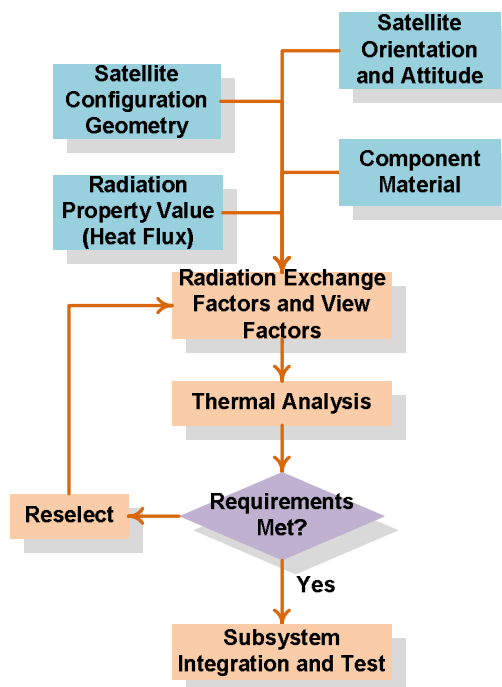


Figure 19. TCS Analysis Flowchart

Considering the CKUSAT configuration, orbit and attitude, the preliminary thermal analyses are executed. The hottest and coldest are in the solar panels (70°C) and satellite adaptor (-20°C), respectively. The temperature range of the key components located in the modules is 0~50°C. Hence, the circuit modules inside CKUSAT can sustain and operate in space environment.

However, the CKUSAT should also do the environment test to confirm the analyses.

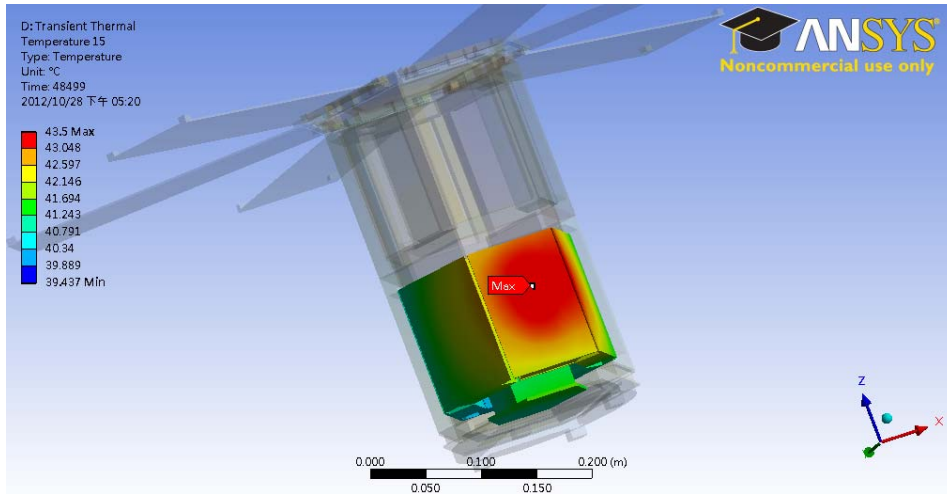


Figure 20. CKUSAT Thermal Analysis Result (Hot Case)

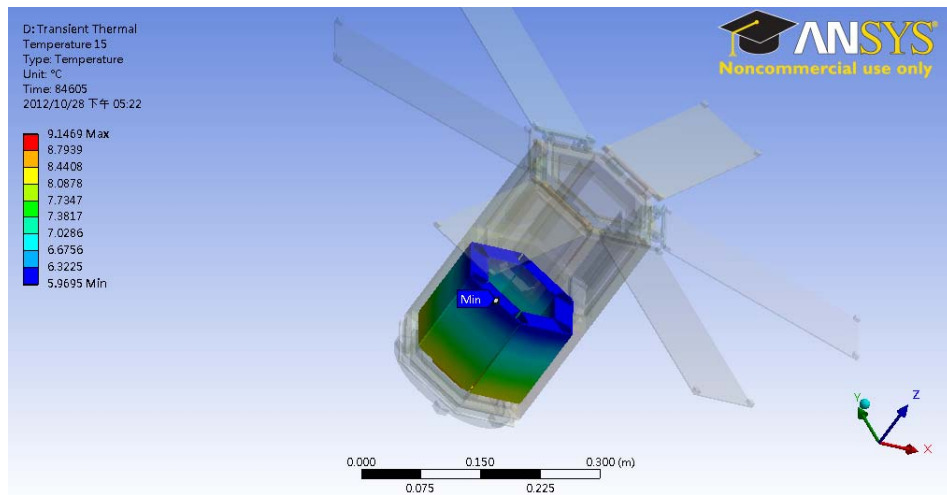


Figure 21. CKUSAT Thermal Analysis Result (Cold Case)

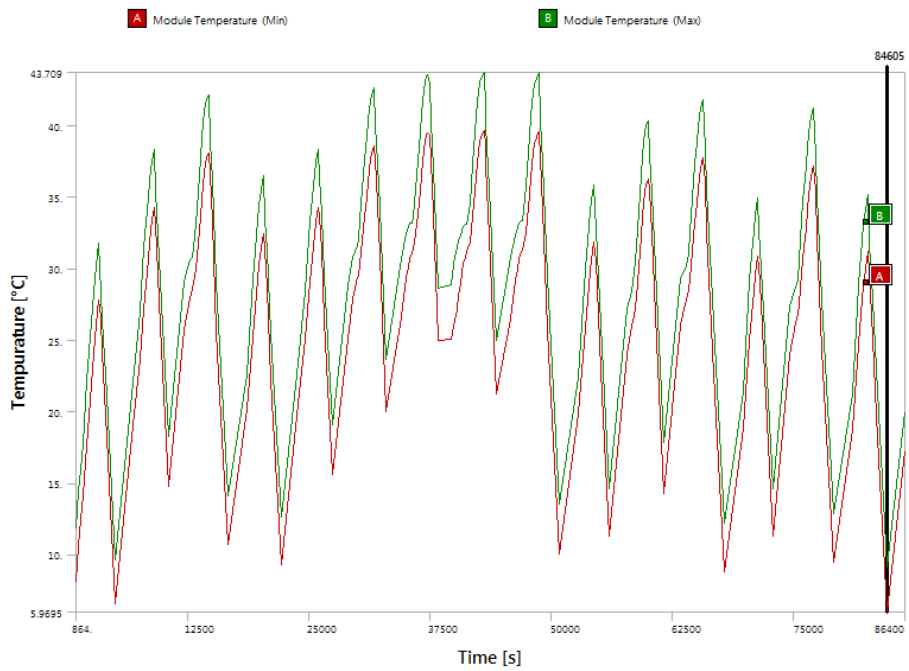


Figure 22. CKUSAT Thermal Analysis Result

Attitude Determination and Control Subsystem (ADCS)

The ADCS consists of a sensor suite that contains sun sensors, a three-axis magnetometer, gyroscope, and GPS receiver payload. The main actuators are three magnetic torque rods and momentum wheels. An onboard processor (32-bit ARM or MCU) runs the attitude determination and control software and interfaces with the sensor and actuators via the ADCS interface board. The ADCS architecture is shown in Figure 23. After satellite separation from launcher, the CKUSAT will perform the B-dot control for satellite detumbling. Figure 24 shows that CKUSAT can settle down from 3 deg/s to 0.5 deg/s within about one orbit period according to the preliminary B-dot control simulation. Because of the requirement of the satellite communication pointing, the CKUSAT also needs three-axis attitude controls by means of momentum wheels. In the beginning of ADCS design, the model testing in simulation will be conducted to verify the feasibility and obtain pertinent design parameters after the establishment of the system specifications and requirements. The Software-In-the-Loop (SIL) test, extensive simulations, is then conducted to verify the control parameters, attitude filters, sensor models, actuator models, and mode switching logics. After that, the hardware platform for real-time control is prepared, designed, and implemented. Afterwards, the Processor-In-the-Loop (PIL) will be employed to verify ADCS hardware and software before the ADCS is integrated into the satellite.

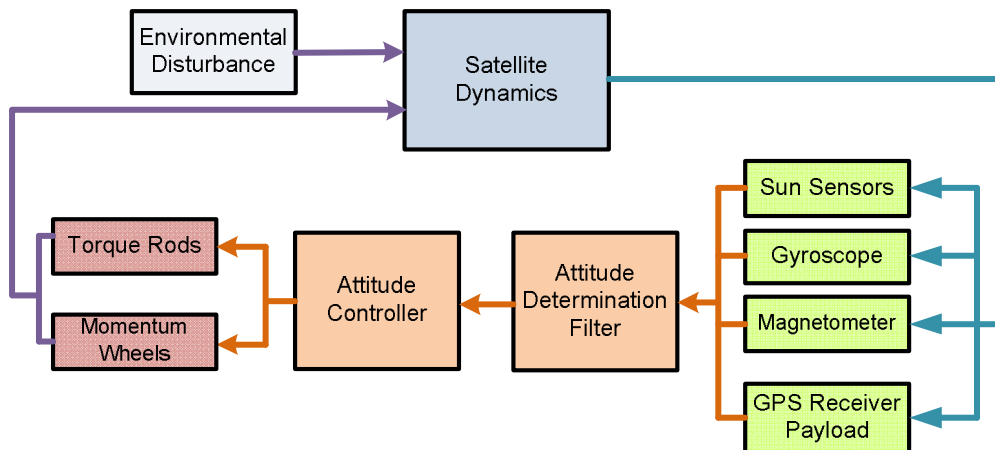


Figure 23. ADCS Architecture

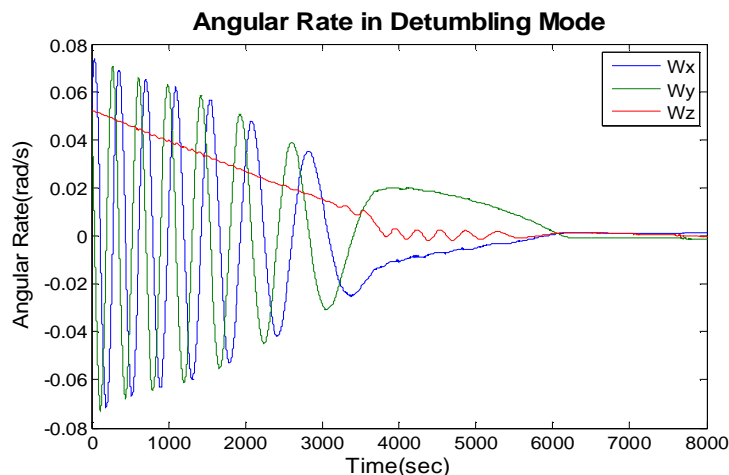


Figure 24. Preliminary B-dot Control Simulation

In addition to the requirement of the satellite communication pointing, the direction of ETP & IP electrode should be aligned with the velocity vector with three-axis stabilization. Hence, the CKUSAT ADCS should be controlled against external disturbances. After the detumbling mode, the CKUSAT will perform the attitude determination via an Extended Kalman Filter (EKF) to provide input for the three-axis stabilization control laws. For the three-axis stabilization control laws, the CKUSAT will implement the momentum biased stabilization.

Electrical Power Subsystem (EPS)

The onboard EPS comprises the Power Distribution and Regulation Unit (PDRU), the battery pack, and a total of 36 body-mounted solar cells. The PDRU is used to distribute regulated power (3.3 Volt and 5 Volt) to satellite bus and payloads. Furthermore, the PDRU with onboard microcontroller is able to measure the bus currents, voltages, and battery status automatically, and send it to C&DH. The battery pack will be connected with a protection circuit to protect against power failures, such as over-charge protection, over-discharge protection, and short-circuit protection. The power of CKUSAT satellite is generated by solar cells during sunlight. The overall schematic of the EPS is illustrated in the following.

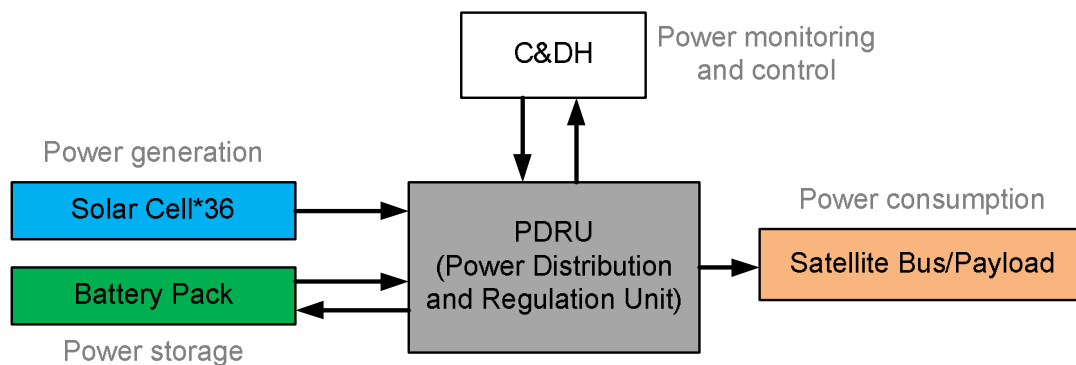


Figure 25. EPS Schematic

Command and Data Handling (C&DH) subsystem

C&DH plays an important role in command validation and execution, data reception, store and downlink, and satellite health maintaining. It also supplies electrical interfaces for subsystems and payloads for transmitting data and issuing/acknowledging commands. The CAN bus is an important interface for the modular design idea, since it is easy to add or remove the satellite bus/payload modules. The Microchip PIC32MX embedded microprocessor would be selected as the main CPU of C&DH, since it has a high performance 32-bit RISC architecture and very low power consumption. The block diagram of the system and its interfaces is shown in Figure 26. In addition, the onboard flight software will be a modular design, which includes four Computer Software Components (CSCs). A CSC is a logical grouping that performs a common function which consists of one or more software units. The CKUSAT CSCs are background monitoring CSC, data collection CSC, data sending CSC and command CSC (Figure 27).

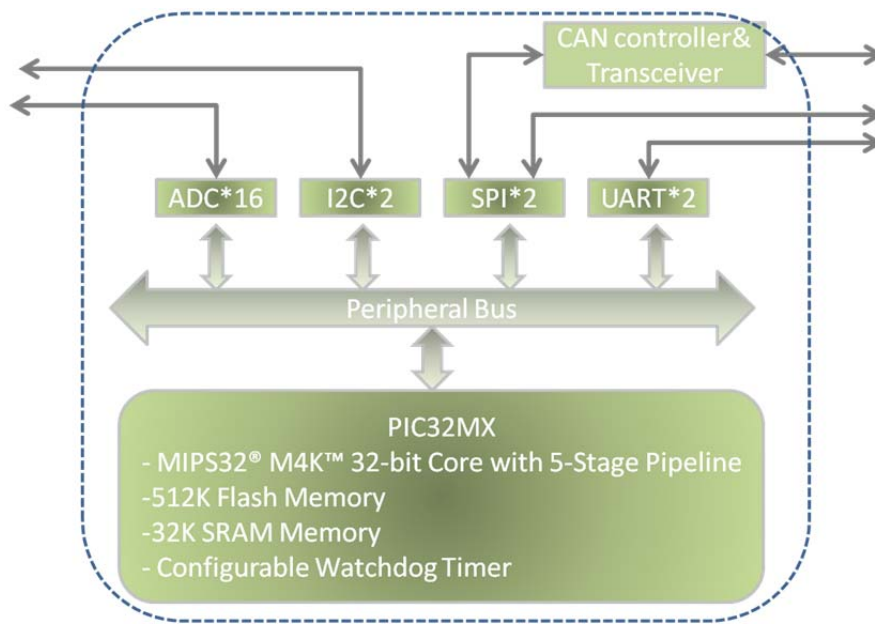


Figure 26. C&DH Block Diagram

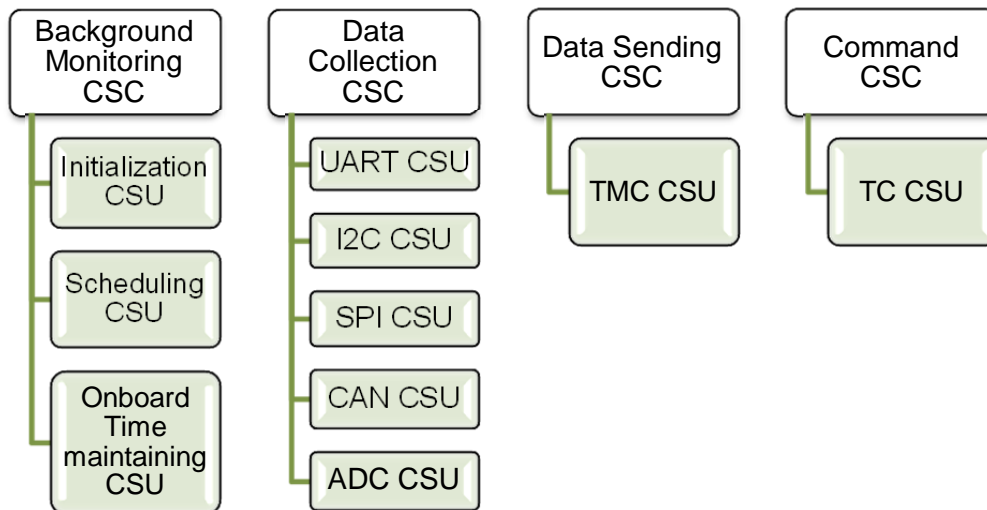


Figure 27. C&DH CSCs Structure

Telemetry, Tracking and Command (TT&C) subsystem

The CKUSAT needs to communicate with the ground station by means of the TT&C subsystem which will use UHF frequency in the amateur radio band to perform beacon broadcasting, telemetry downlink, and telecommand uplink. The TT&C will send a periodic Morse code beacon for satellite tracking and health reporting. For the link protocol, the AX.25 telemetry protocol will be implemented with 9600bps data rate and the telecommand will be selected to the self-made protocol. Figure 28 shows the TT&C operation procedure. When CKUSAT is in the field of view of ground station, the telemetry and telecommand tasks will be executed. On the other hand, when the satellite is out of the field of view of ground station, the CKUSAT broadcasts beacon to supply the other ground stations to track CKUSAT.

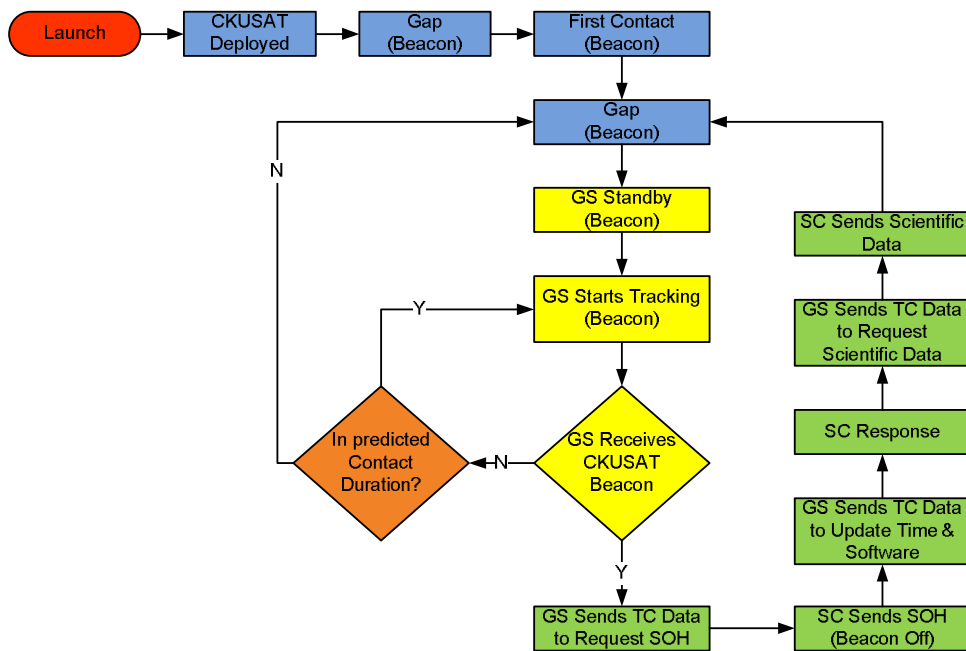


Figure 28. TT&C Operation Procedure

Table 5. Telemetry Download Capability Analysis

Data Type	Data Length (bits)	Sampling Interval (Sec)	Total Data Length (byte)
Subsystems Data			303,354
ADCS	360	1	280980
EPS	240	60	3122
TCS	40	60	520
C&DH	24	1	18732
Payloads Data			2,713,018
ETP	1600	1	1248800
IP	1600	1	1248800
VLF	80	1	62440
GPSR	196	1	152978
Total			3,016,372
Note: Orbit Period 6244 seconds [Margin Factor: 1.1]			
	Data Rate	Average Pass Duration (sec)	
TT&C download capability	9600	630	756,000
ECP download capability	38400	630	3,024,000

Electron Temperature Probe (ETP) payload

The ETP system was invented by K. I. Oyama and his collaborators about 40 years ago in Japan. The ETP system has advantages not only as being small and light weighted, but also being able to give accurate measurement of electron temperature. ETP takes advantage of probe floating potential shifts in plasma with applying RF sinusoidal signal (30 kHz) of two different amplitudes “a” and “2a” on probe. The ETP circuit block diagram is shown as Figure 29. This system consists of RF signal oscillator of 30 kHz, wave modulator to produce the two amplitudes, DC differential amplifier, and PCM interface if needed.

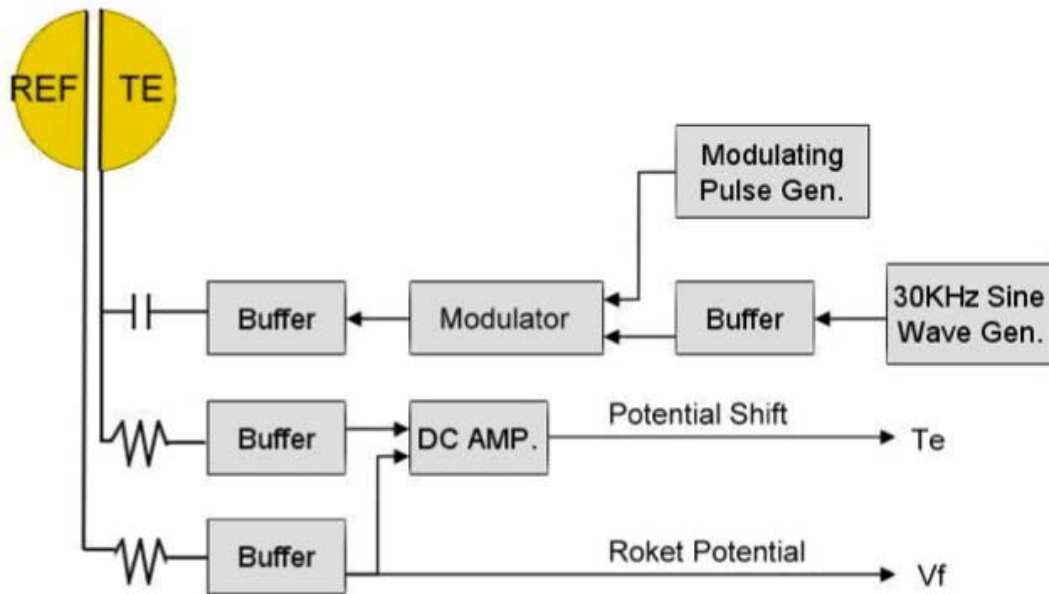


Figure 29. ETP Circuit Block Diagram

Period of the applied and measured signal is one second (Figure 30). Electron temperature can be derived from ratio of DC voltage level, and electron density can also be derived with considering plasma sheath effect and fit the measure curve in some density range (roughly $10^9 \sim 10^{11} \text{ cm}^{-3}$). Density measured by ETP can also be a reference of density measured by IP. Least sampling rate of ETP is 100 samples per second.

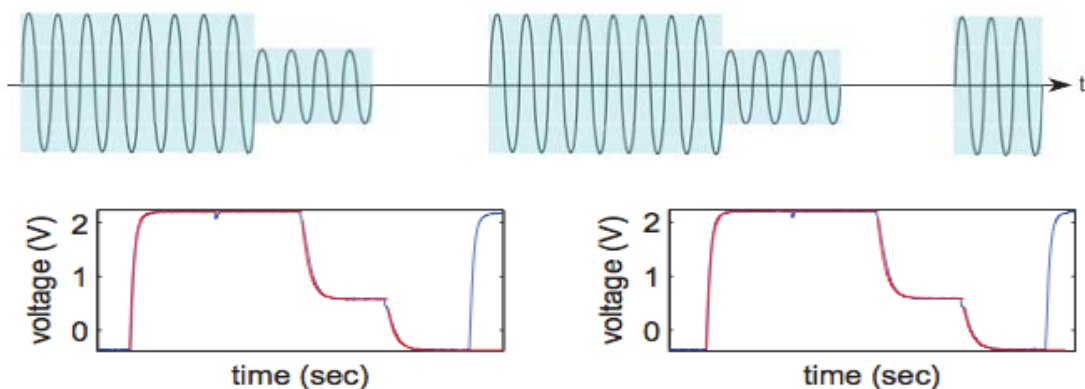


Figure 30. Examples of the Applied Signal and Measured Raw Data of ETP

An example of ETP data product is shown as Figure 31. For the first year of CKUSAT mission, we need to develop the model of global electron temperature profile. Then we can use the model as a reference of electron temperature. These kinds of diagrams should be plotted from downloaded satellite raw data instantly. Then people can realize electron temperature variations in case of earthquake precursor events occur easily.

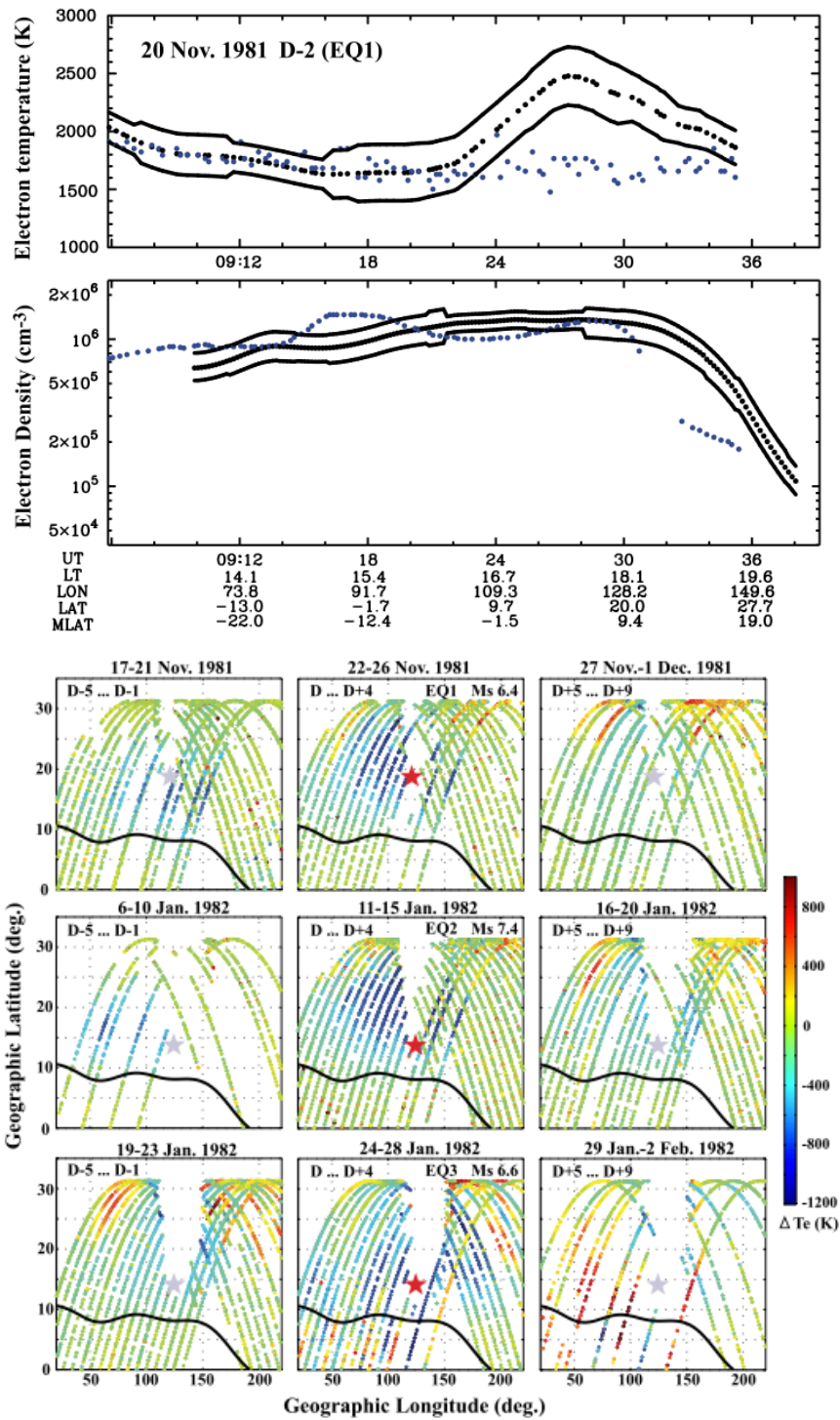


Figure 31. Examples of ETP Data Product

Considering electron density and temperature range of ionosphere at 500km, ETP electrode size is decided 10cm-diameter circular plane (Figure 32).

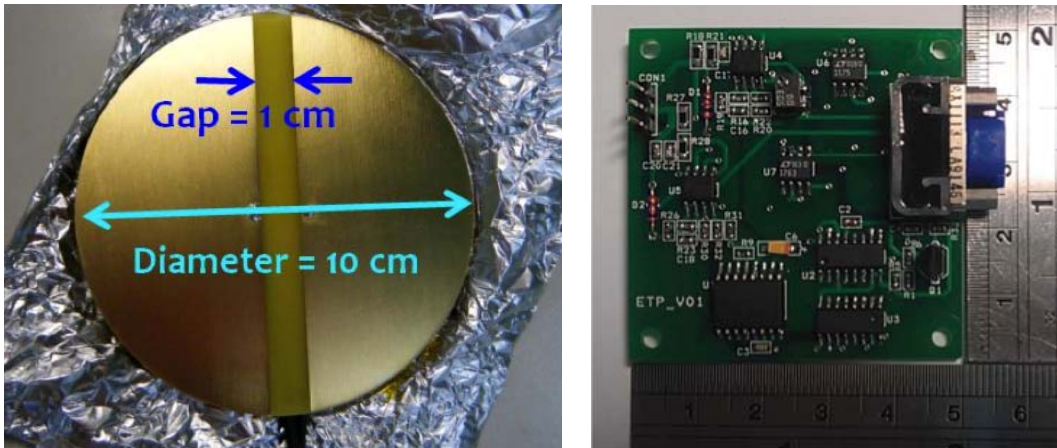


Figure 32. Picture of the ETP Electrode and Circuit Board

Impedance Probe (IP) payload

The impedance probe (IP) system is a powerful instrument for electron density measurement in sake of its ability to derive absolute electron density. Several plasma resonance modes with EM waves (which relate to electron density) can be found with applying a sweeping-frequency signal on antenna and finding antenna impedance singularities. The IP transmits electrostatic waves from the probe into the plasma to find the Upper Hybrid Resonance (UHR) by sweeping a wide range of frequencies (500kHz – 12MHz). IP is independent of the electrode contamination and can provide high accuracy for electron density measurement.

The ETP electrode is used for the IP antenna with switch circuit. By finding the upper hybrid resonance frequency at which current at antenna is singularity (Figure 34), electron density can be derived. Least sampling rate of IP is 100 samples per second.

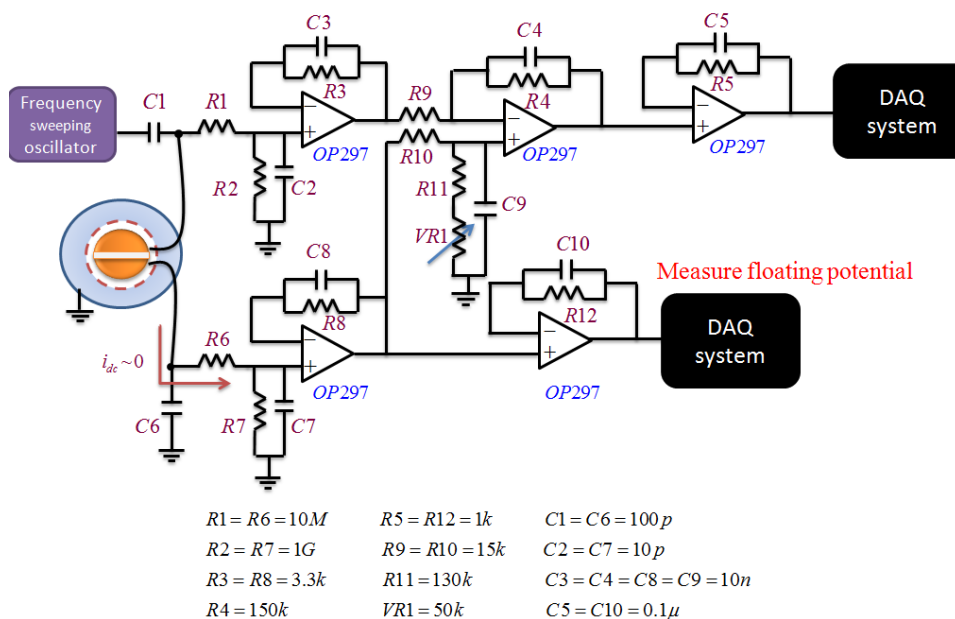


Figure 33. IP Circuit Diagram

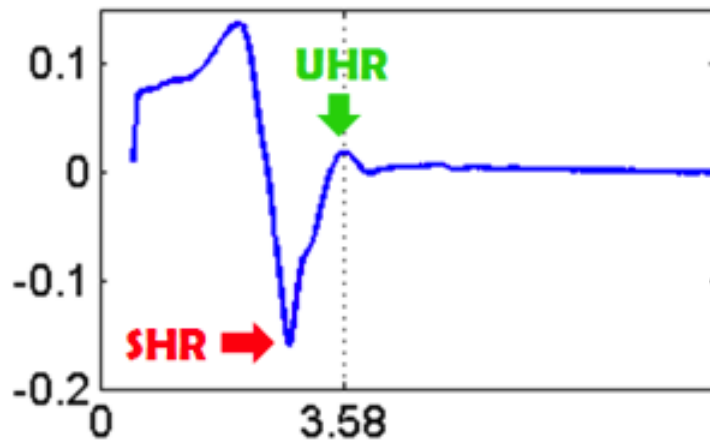


Figure 34. Examples of the measured raw data of IP (Upper hybrid resonance at 3.58 MHz)

Same as ETP, IP data product (Figure 35) should also be plotted from downloaded raw data instantly after a one-year electron density model is developed.

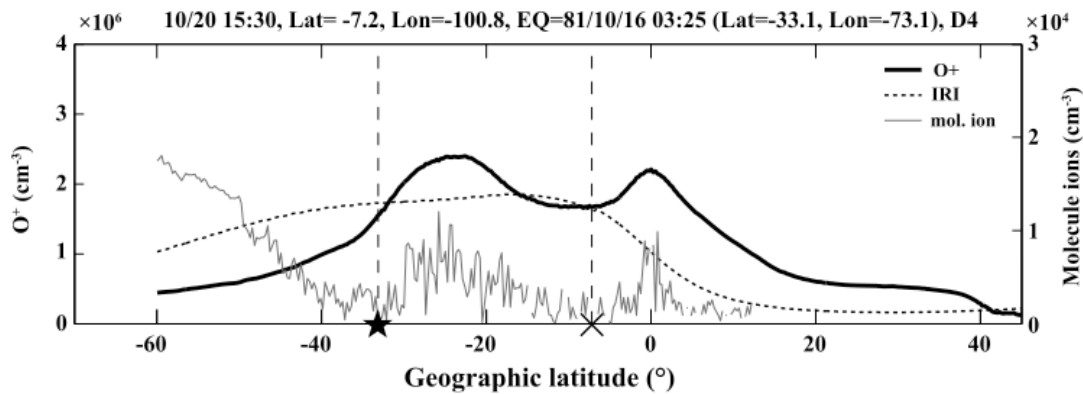


Figure 35. Examples of IP Data Product

Very-Low Frequency sensor (VLF) payload

The VLF sensor is positioned in the top panel of the CKUSAT to measure the earth magnetic field in very low frequency range which is less than 10 KHZ. The VLF system will consist of thousands turns diameter coils which are a search coil and a calibration coil, and an amplifier/filter circuit (Figure 36). Although it can be switched on by C&DH as satellite passing by earthquake hotspots, CKUSAT should plan to operate it continuously for in the mission.

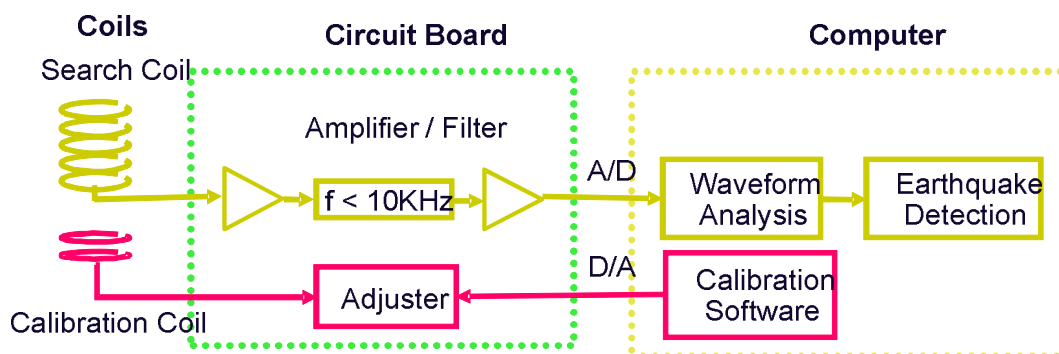


Figure 36. VLF Schematic

GPS Receiver (GPSR) for space application

GPS is a popular navigation system so that more and more satellites equip an onboard GPS receiver for orbit determination. A GPS receiver for space application differs from a commercial GPS receiver as the satellite high dynamics gives rise to the high Doppler shifts and Doppler shift rates. Since the purchase of space-qualified GPS receiver is subject to budget and export control restrictions, to develop the space-borne GPS receiver indigenously is required. A domestic onboard GPS receiver will be developed to verify the navigation functions and performance in space environment. In the development of the GPSR payload, the signal characteristics such as visibility and Doppler shift with respect to GPS satellites will be analyzed. Afterward, the GPSR firmware/software are developed and implemented accordingly to meet the requirement of signal tracking in the high dynamic environment. The software consists of orbit propagator, Kalman filter, tracking loop control, visibility computing, ephemeris management, data demodulation and measurement processing (Figure 37). NCKU team has developed a space application GPS receiver prototype (Figure 38).

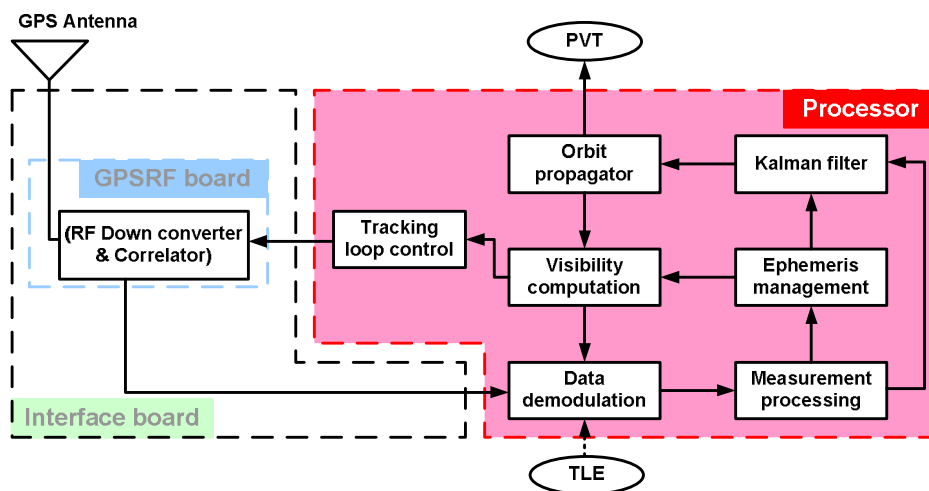


Figure 37. GPSR payload System Diagram



Figure 38. GPSR Payload Prototype

Experiment for Communication Payload (ECP)

ECP is the other onboard experimental payload on CKUSAT. Its mission is to execute the communication in 2.4GHz (S-band) to know its performance. Afterward, the result will be an important reference for further microsatellite with 2.4GHz communication. Although the scientific data can be downloaded via the CKUSAT TT&C subsystem UHF band, the data volume is limited. Hence, higher data rate downlink is essential for the CKUSAT earthquake mission. The hardware of ECP includes a transceiver module and patch antenna. The transceiver module will implement Texas Instrument CC2500 chip and RF amplifier. The patch antenna is located on the bottom face of CKUSAT satellite. The link budget of ECP communication with data rate 20000bps is shown in the following.

Table 6. EPC Downlink Budget

Parameter:	Value:	Units:
<i>Spacecraft:</i>		
Transmitter Power Output:	2.20	watts
	In dBW:	3.42 dBW
	In dBm:	33.42 dBm
Transmission Line Losses:	-0.2	dB
Connector, Filter or In-Line Switch Losses:	-1.0	dB
Antenna Gain:	9.00	dBiC
Satellite EIRP:	11.22	dBW
<i>Downlink Path:</i>		
Satellite Antenna Pointing Loss:	-7.0	dB
Antenna Polarization Losses:	0.0	dB
Path Loss:	-163.56	dB
Atmospheric Losses:	-0.5	dB
Ionospheric Losses:	-0.01	dB
Rain Losses:	0.0	dB
Isotropic Signal Level at Ground Station:	-159.85	dBW
<i>Ground Station:</i>		
<i>----- Eb/No -----</i>		
Ground Station Antenna Pointing Loss:	-3.0	dB
Ground Station Antenna Gain:	24	dBiC
Ground Station Transmission Line Losses:	-0.5	dB
Ground Station LNA Noise Temperature:	66.7779435	K
Ground Station Transmission Line Temp.:	290	K
Ground Station Sky Temperature:	450	K
S/C Transmission Line Coefficient:	0.8913	
Ground Station Effective Noise Temperature:	499	K
Ground Station Figure of Merit (G/T):	-3.5	dB/K
S/C Signal-to-Noise Power Density (S/No):	62.3	dBHz
System Desired Data Rate:	38400	bps
	In dBHz:	45.8 dBHz
Telemetry System Eb/No:	16.4	dB
Telemetry System Required Bit Error Rate:	1.00E-05	
Telemetry System Required Eb/No:	13.4	dB
System Link Margin:	3.0	dB

2.3 Ground Segment

The ground segment elements of CKUSAT are illustrated in Figure 39. NCKU Ground Station (GS) is used to be the primary ground station site, which is located at 22.56.17N / 120.16.38E and Height 31 meters. When CKUSAT operates in orbit, the satellite needs to communicate with GS. GS needs to uplink commands to the satellite and receive the scientific data and SOH (Status Of Health) from the satellite. The responsibility of the Mission Operations System (MOS) is to keep the satellite in healthy condition and carry out operations to achieve the mission objectives. The MOS would support analysis of the satellite's health status from satellite telemetry, update/synchronize the onboard time, payload experimental task scheduling. The MOS will also archive all CKUSAT mission data for further analysis and next satellite design reference. Moreover, the downlinked data,

in particular, the key technical and scientific data, will be analyzed to yield engineering and scientific values. Therefore, all downlinked data will be stored in the data center and analyzed by NCKU team. Furthermore, since the ultimate mission objective is to form an earthquake precursor constellation, the data will be shared and exchanged with joint satellite teams to accelerate global earthquake study.

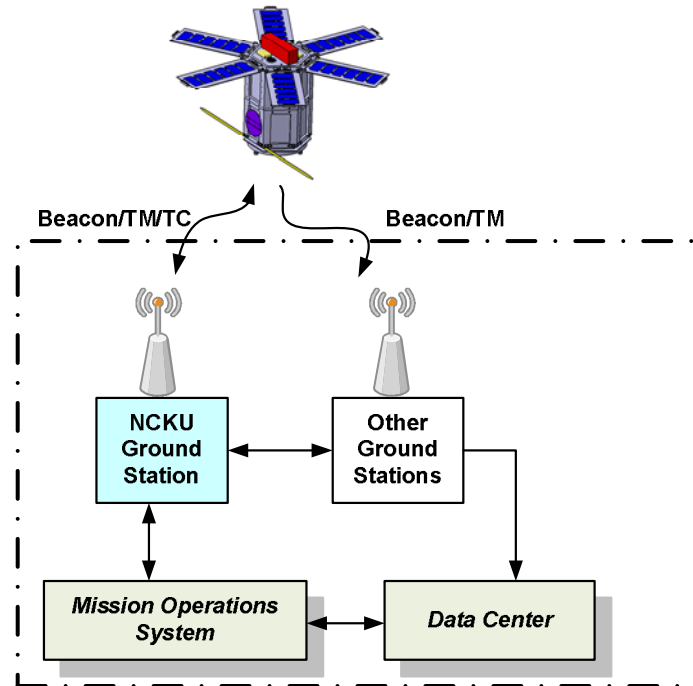


Figure 39. Ground Segment Elements

3. Anticipated Results

The CKUSAT microsatellite will be an experimental platform to collect data for earthquake study after it is launched. Besides, CKUSAT satellite is a modular design so that it is easy to duplicate or extend more and more satellites to construct a constellation and join the earthquake research. Data sharing among these constellation members will accelerate to build up the earthquake precursor warning system. In addition to the technical benefits, the earthquake subject might be a good scientific topic for students to learn. The CKUSAT mission is also aimed to provide a good tool for education and train space related engineering.

4. Originality and/or social effects

Through the design and manufacturing of CKUSAT microsatellite, participating students have the opportunity to gain hands-on experiences in satellite analysis, design, assembly, and test. Moreover, these students will have many opportunities to interact with engineers from national laboratory, domestic industry, and international companies. Some international students would be invited to join the development of the CKUSAT project so that the domestic students could cooperate with foreign students and exchange different thoughts. This will pave the way for the outstanding space technology in Taiwan. The CKUSAT project is expected to provide valuable output in terms of satellite engineering knowledge, with the aim to establish a national center at

NCKU for the development of satellites. Furthermore, the CKUSAT will be a pioneer of earthquake precursor constellation in order to attract other universities or private agencies to join international cooperation for earthquake research and satellite development.

5. Concrete achievement methods, range and budget for manufacturing

This CKUSAT development will has been undertaken by the NCKU team, coordinated by several NCKU departments. During the satellite development, NCKU will make good use of man power, existing equipments and facilities to conduct and validate satellite development. The available equipments and facilities are space plasma chamber (2m in diameter and 3m in length), Class 100K clean booth, 130 keV ion beam system, temperature & humidity test chamber, network analyzer, spectrum analyzer, signal generator, oscilloscope, NI-PXI for satellite hardware development, and Matlab, LabVIEW, and ANSYS software for satellite analysis and simulation. The preliminary cost is listed in the following. The preliminary estimated budget is about 0.2 million US dollars for a single satellite development and manufacture.

Table 7. Cost Breakdown

Core Components	
Structure	15,000
TT&C Transceiver	30,000
Solar Panel	48,000
PDRU	18,000
ADCS Sensors	30,000
ADCS momentum wheels	21,000
ADCS Torque rods	18,000
C&DH	9,000
Misc	10,000
Total	199,000

6. Development, manufacture and launch schedule

The development of CKUSAT is expected to be completed within three years. The design review meetings are necessary during the satellite development. After kick-off meeting, the satellite requirement definition, element specification definition, design analysis and satellite bus/payloads architecture design will be conducted. Before preliminary design review (PDR), the key components in purchase process will be acquired and put into implement. Flight software coding will start at the same time with onboard hardware implement and installation. Before critical design review (CDR), the integration and test of the CKUSAT hardware and software will be in process and expected to be completed soon. After that, the complete satellite will be assembly and integrated by NCKU team. In addition, the environment test will be conducted after the integration and test review (ITR). Whenever applicable, a launch vehicle (LV) interface meeting should be held with the LV provider to discuss and define the interface between CKUSAT and LV. At last, the CKUSAT is ready to ship to

launch site and integrate with launch vehicle. After CKUSAT launched, it is expected that the CKUSAT satellite can operate in space for three years for earthquake precursor mission.

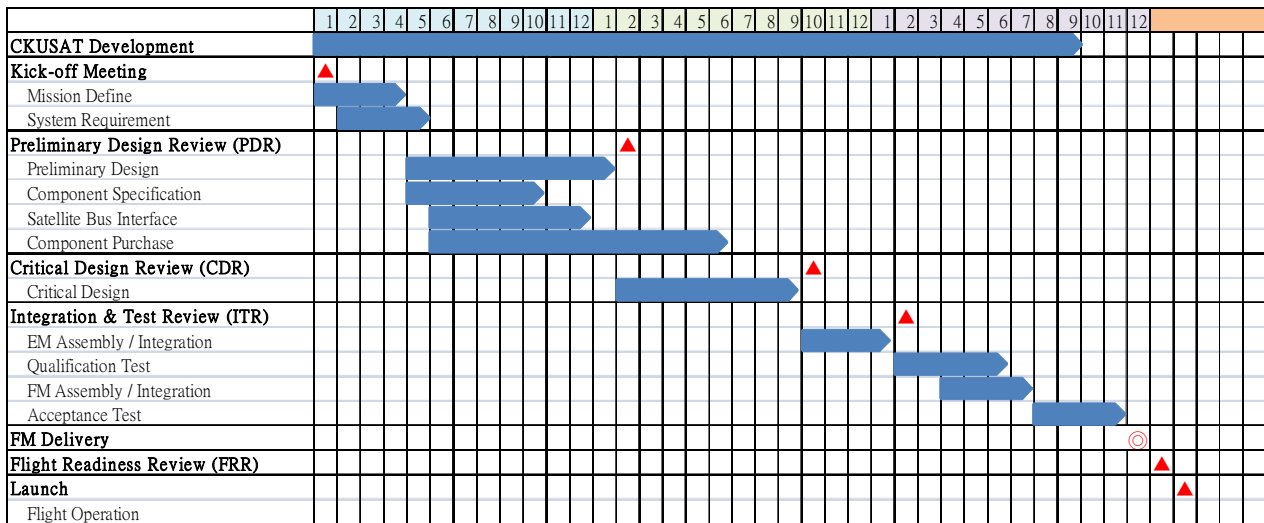


Figure 40. CKUSAT Development Schedule

7. Conclusion

The CKUSAT mission aims to focus on earthquake precursor observation from space. It will carry VLF, ETP, and IP payloads, to detect very low frequency signals and measure the electron temperature and density due to earthquake. In addition to the earthquake research, the NCKU team will perform the mission design, trade-off analysis, system design, subsystem design and payload design. It will intend to encourage the space engineering education and engineering application for participated students to gain hands-on experience. Most important, the CKUSAT can be regarded as a pioneer to encourage universities or private agencies to cooperate together for earthquake precursor.

References

- [1] Y. Y. Ruzhin, V. A. Larkina, and A. K. Depueva, "Earthquake precursors in magnetically conjugated ionosphere regions," *Adv. Space Res.*, 21, 525-528, doi:10.1016/S0273-1177(97)00892-2, 1998.
- [2] T. Ondoh, "Seismo-ionospheric phenomena," *Adv. Space Res.*, 26(8), 1267-1272, doi:10.1016/S0273-1177(99)01215-6, 2000.
- [3] A. A. Silina, E. V. Liperovskaya, V. A. Liperovsky, and C. -V. Meister, "Ionospheric phenomena before strong earthquakes," *Nat. Hazards Earth Syst. Sci.*, 1, 113-118, doi:10.5194/nhess-1-113-2001, 2001.
- [4] J. Y. Liu, Y. I. Chen, Y. J. Chuo, and H. F. Tsai, "Variation of ionospheric total electron content during the Chi-Chi earthquake," *Geophys. Res. Lett.*, 28, 1383-1386, doi: 10.1029/2000GL012511, 2001.

- [5] J. Y. Liu, Y. J. Chuo, S. J. Shan, Y. B. Tsai, Y. I. Chen, S. A. Pulinets, and S. B. Yu, "Pre-earthquake ionospheric anomalies registered by continuous GPS TEC measurements," *Ann Geophys.*, 22, 1585-1593, doi:10.5194/angeo-22-1585-2004
- [6] S. Pulinets and K. Boyarchuk, *Ionospheric Precursors of Earthquakes*, Springer, New York, 2004
- [7] M. Devi, A. K. Barbara, and A. Depeuva, "Association of total electron content (TEC) and foF2 variations of earthquake events at the anomaly crest region," *Ann. Geophys.*, 47(1), 83-91, 2004.
- [8] M. Parrot, J. -J. Berthelier, J. P. Lebreton, J. A. Sauvaud, O. Santolik, and J. Bleski, "Examples of unusual ionospheric observations made by the DEMETER satellite over seismic regions," *Phys. Chem. Earth*, 31, 486-495, 2006.
- [9] D. K. Sharma, M. Israil, R. Chand, J. Rai, P. Subrahmanyam, and S. C. Garg, "Signature of seismic activities in the F2 region ionosphere electron temperature," *J. Atmos. Sol. Terr. Phys.*, 68, 691-696, doi:10.1016/j.jastp.2006.01.005, 2006.
- [10] K. I. Oyama, Y. Kakinami, J. Y. Liu, M. Kamogawa, and T. Kodama, "Reduction of electron temperature in low-latitude ionosphere at 600 km before and after large earthquakes," *J. Geophys. Res.*, 113, A11317, doi:10.1029/2008JA013367, 2008.
- [11] L. G. Bankov, M. Parrot, R. A. Heelis, J. -J. Berthelier, P. G. Marinov, and A. K. Vassileva, "DEMETER and DMSM satellite observations of the disturbed H⁺/O⁺ ratio caused by Earth's seismic activity in the Sumatra area during December 2004," *Adv. Space Res.*, 46, 419-430, doi:10.1016/j.asr.2009.07.032, 2010.
- [12] T. Dautermann, E. Calais, J. Hasse, and J. Garrison, "Investigation of ionospheric electron content variations before earthquakes in southern California," 2003-2004, *J. Geophys. Res.*, 112, B02106, doi:10.1029/2006JB004447, 2007.
- [13] S. A. Pulinets, and M. A. Dunajecka, "Specific variations of air temperature and relative humidity around the time of Michoacan earthquake M8.1 Sept. 19, 1985 as a possible indicator of interaction between tectonic plates," *Tectonophysics*, 431, 221-230, doi:10.1016/j.tecto.2006.05.044, 2007.
- [14] B. Zhao, T. Yu, M. Wang, J. Lei, and B. Ning, "Is a usual large enhancement of ionospheric electron density linked with the 2008 great Wenchuan earthquake? ," *J. Geophys. Res.*, 113, A11304, doi:10.1029/2008JA013613, 2008.
- [15] J. Y. Liu, et al., "Seismo-ionospheric GPS TEC anomalies observed before the 12 May 2008 M7.9 Wenchuan earthquake," *J. Geophys. Res.*, 114, A04320, doi:10.1029/2008JA013698, 2009.
- [16] S. A. Pulinets, V. G. Bondur, M. N. Tsidilina, and M. V. Gaponova, "Verification of the concept of seismoionospheric coupling under quiet Heliogeomagnetic conditions, using the Wenchuan (China) earthquake of May 12, 2008," as an example, *Geomagn. Aeron.*, 50(2), 231-242, doi:10.1134/S0016793210020118, 2010.

- [17] K. I. Oyama, Y. Kakinami, J. Y. Liu, C. Y. Chen, and T. Kodama, "Micro/Mini Satellites for Earthquake Studies - Toward International Collaboration -," *Advances in GeoSciences*, Vol. 21, ST, 251-275, 2010.
- [18] K. I. Oyama, J. Y. Liu, Y. Kakinami, and T. Kodama, "Constellation of Micro Satellites for Earthquake Study - Toward International Collaboration," *Asian Space Conference*, Taipei, 2008.
- [19] T. Kodama and K. I. Oyama, "The ELMOS Small Satellite Constellation," *The 28th International Symposium on Space Technology and Science*, Okinawa, June 5-12, 2011.
- [20] K. I. Oyama, Y. Kakinami, J. Y. Liu, M. A. Abdu, and C. Z. Cheng, Latitude distribution of anomalous ion density as a precursor of a large earthquake, *J. Geophys. Res.*, 116, A04319, doi:10.1029/2010JA015948, 2011.
- [21] A. Rozhnoi, M. Solovieva, O. Molchanov, P. -F. Biagi, and M. Hayakawa, Observation evidences of atmospheric gravity waves induces by seismic activity from analysis of subionospheric LF signal spectra, *Nat. Hazards Earth Syst. Sci.*, 7, 625-628, doi:10.5194/nhess-7-625-2007, 2007
- [22] K. I. Oyama, "Technical information of Electron temperature probe (ETP)," ETP TEC2008-3/11.
- [23] K. I. Oyama, "Instruction Manual to check Electron temperature probe (ETP)," ETP MAN2008-3/14.
- [24] J. C. Juang and J. J. Miao, "Overview of the PACE satellite: a Three-Axis Stabilized CubeSat", first International CubeSat. Symposium, Japan, 2003
- [25] J. K. Tu, S. H. Wu, and C. C. Chu, "Platform for Attitude Control Experiment (PACE) An Experimental Three-Axis Stabilized CubeSat" - National Cheng Kung University," *Proc. 18th AIAA/USU Conference on Small Satellites, SSC-VII*, Utah State University, Logan Utah, USA, August 9-12, 2004.
- [26] J. J. Miao and J. C. Juang, "A University Nano-Satellite Program: PACESAT", 5th IAA Symposium on Small Satellites for Earth Observation, IAA-B5-0 510P, Berlin, Germany, April 4 - 8, 2005.
- [27] J. C. Juang, J. J. Miao, Y.Y. Liu, and B. C. Chen "Earthquake Research from Space: LEAP Microsatellite Design in Taiwan," *Asian Space Conference*, Singapore, 2007.
- [28] J. J. Miao and J. C. Juang, "LEAP: A Student Microsatellite Design Project", *Proc. iNEER Conference for Engineering Education and Research*, Melbourne, 2007.
- [29] J. C. Juang, Y. F. Tsai, and J. J. Miao, 'Status Update of the LEAP Micro-Satellite,' *Asian Space Conference*, Taipei, 2008.
- [30] J. C. Juang, Y. F. Tsai, and C. T. Tsai, "Design and verification of a magnetometer-based orbit determination and sensor calibration algorithm," *Aerospace Science and Technology*, doi:10.1016/j.ast.2011.05.003, 2011.
- [31] Y. F. Tsai, C. C. Chang, J. C. Juang, and C. T. Lin, "Implementation and Test of a Space-borne GPS Receiver Payload of Micro Satellite," *International Symposium on GPS/GNSS 2010 Proceedings*, Taiwan, 2010.

- [32] A. Scholz, J. J. Miao, J. C. Juang, and H. L. Chiu, "Development of Miniature Digital Sun Sensors at NCKU," presented at the 4th Asian Space Conference & Formosat-3/COSMIC International Workshop, Taipei, 2008.
- [33] J. C. Juang, Y. F. Tsai, C. T. Tsai, S. T. Jenq, J. R. Tsai, and H. P. Pan, "Taiwan Experimental Microsatellite Project - CKUTEX," presented at the 8th IAA Symposium on Small Satellites for Earth Observation, Berlin, Germany, 2011.
- [34] J. C. Juang, Y. F. Tsai, C. T. Tsai, S. T. Jenq, J. R. Tsai, and H. P. Pan, "CKUTEX – An Experimental Microsatellite by NCKU," 2010 AASRC Conference Proceedings, Taoyuan, Taiwan, 2010.
- [35] J. C. Juang, Y. F. Tsai, C. T. Tsai, S. T. Jenq, J. R. Tsai, C. R. Chen, and H. P. Pan, "Development and Test of the CKUTEX Microsatellite," *Journal of Aeronautics, Astronautics and Aviation, Series A*, Vol.43, No.3, pp.219 - 228, 2011.